previously (18). All mice were maintained under specific pathogen-free conditions in the Animal Facility of the Hokkaido University Graduate School of Medicine (Sapporo, Japan). Animal experiments were conducted according to the guidelines established by the Animal Safety Center, Japan.

Cell lines and reagents

Human hepatocyte cell lines O cells and O cured (Oc) cells that contained HCV 1b replicons were provided by N. Kato (Okayama University). Mouse hepatocyte cell line was described previously (19). PolyI:C was purchased from GE Healthcare and dissolved in saline. An OVA (H2K^b-SL8) tetramer was purchased from MBL. PE-CD80, -CD86, -NK1.1, FITC-CD8, and allophycocyanin-CD3e Abs were purchased from BioLegend, and PE-CD40, FITC-CD69, and allophycocyanin-CD11c Abs were from eBioscience. An ELISA kit for IFN-β was purchased from PBL Biomedical Laboratories, and ELISA kits for mouse IL-28 (IFN-λ2/3) were purchased from Abcam and eBioscience. An ELISA kit for mouse IFN-γ was purchased from eBioscience. ELISA was performed according to the manufacturer's instructions. Mouse IFN-α and IFN-λ3 (IL-28B) were purchased from Miltenyi Biotec and R&D Systems, respectively.

Cell preparation

Spleen CD8$^+$ and CD4$^+$ DCs were isolated using CD8$^+$ DC isolation kit and CD4-positive isolation kit, according to manufacturer's instruction (Miltenyi Biotec). Spleen CD11c$^+$ DCs were isolated using CD11c microbeads. To obtain splenic double-negative (DN) DCs, CD4$^+$ and CD8$^+$ cells were depleted from mouse spleen cells using CD4 and CD8 MicroBeads (Miltenyi Biotec), and then CD11c$^+$ DCs were positively selected using CD11c MicroBeads (Miltenyi Biotec). We confirmed that >90% of isolated cells were CD4$^-$, CD8$^-$, and CD11c$^+$ DCs. Splenic NK cells were isolated using mouse DX5 MicroBeads (Miltenyi Biotec). The cells were analyzed by flow cytometry on a FACSCalibur instrument (BD Biosciences), followed by data analysis using FlowJo software.

Generation of bone marrow–derived DCs and bone marrow–derived macrophages

Bone marrow cells were prepared from the femur and tibia. The cells were cultured in RPMI 1640 medium with 10% FCS, 100 μM 2-ME, and 10 ng/ml murine GM-CSF or culture supernatant of L929 expressing M-CSF. Medium was changed every 2 d. Six days after isolation, cells were collected.
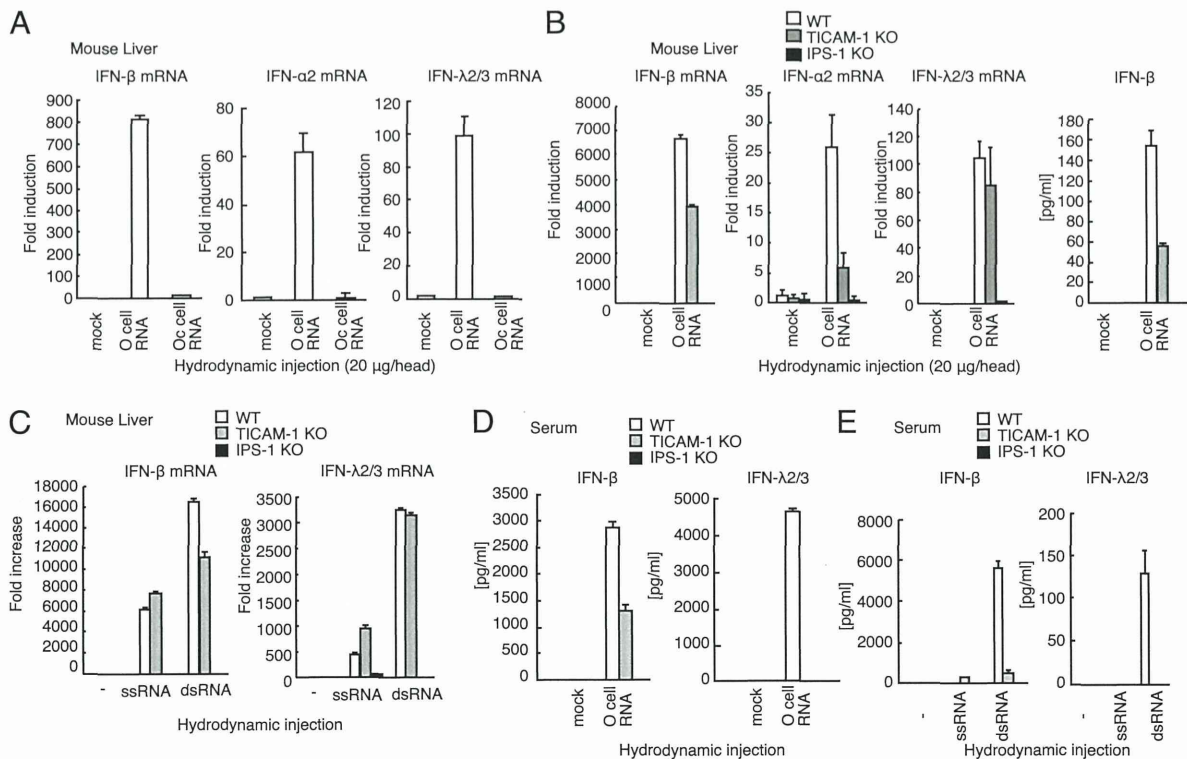
Hydrodynamic injection

Total RNA from the human hepatocyte cell lines O cells and Oc cells was extracted using TRIzol reagent (Invitrogen). HCV genotype 1b 3′ UTR RNA, including the polyU/UC region, was synthesized using T7 and SP6 RNA polymerase and purified with TRIzol, as described previously (20). RNA was i.v. injected into a mouse by a hydrodynamic method using a TransIT Hydrodynamic Gene Delivery System (Takara), according to the manufacturer's instruction.

Quantitative PCR

For quantitative PCR, total RNA was extracted using TRIzol reagent (Invitrogen), after which 0.1–1 μg RNA was reverse transcribed using a high-capacity cDNA transcription kit with an RNase inhibitor kit (Applied Biosystems), according to the manufacturer's instructions. Quantitative PCR was performed using a Step One real-time PCR system (Applied Biosystems). The expression of cytokine mRNA was normalized to that of β-actin mRNA, and the fold increase was determined by dividing the expressions in each sample by that of wild type at 0 h. PCR primers for mouse IFN-λ amplified both IFN-λ2 and λ3 mRNA. The primer sequences are described in Supplemental Table 1.

Activation of NK cells in vitro

NK cells and CD11c$^+$ DCs were isolated from spleens using DX5 and CD11c MicroBeads (Miltenyi Biotec), respectively. A total of 2×10^5 NK

FIGURE 1. Type I and type III IFN productions in response to HCV RNA in vivo. (**A**) O cell and Oc cell RNA (20 μg) were hydrodynamically injected into wild-type mice. Six hours later, mouse livers were excised, and IFN-β, α2, and -λ2/3 mRNA levels were determined by quantitative RT-PCR. (**B**) O cell RNA (20 μg) with HCV replicons was hydrodynamically injected into wild-type, TICAM-1 KO, and IPS-1 KO mice. Six hours after injection, IFN-β, α2, and -λ2/3 mRNA levels in liver were determined by quantitative RT-PCR. IFN-β protein levels in mouse livers were determined by ELISA. (**C**) HCV ssRNA or HCV dsRNA (5 μg) was hydrodynamically injected into wild-type, TICAM-1 KO, and IPS-1 KO mice. Six hours after injection, IFN-β and -λ2/3 mRNA levels in liver were determined by quantitative RT-PCR. (**D**) O cell RNA (20 μg) with HCV replicons was hydrodynamically injected into wild-type, TICAM-1 KO, and IPS-1 KO mice. Six hours after injection, serum IFN-β and -λ2/3 concentrations were determined by ELISA. (**E**) HCV ssRNA or HCV dsRNA (5 μg) was hydrodynamically injected into wild-type, TICAM-1 KO, and IPS-1 KO mice. Six hours after injection, serum IFN-β and -λ2/3 concentrations were determined by ELISA.

cells and 1×10^5 DCs was cocultured with IFN-λ, IFN-α, or polyI:C. After 6, 12, and 24 h, IFN-γ concentrations in the supernatants were determined by ELISA. To determine CD69 expression, NK1.1$^+$ and CD3e$^+$ cells in 24-h sample were gated.

Ag-specific T cell expansion in vivo

OVA (1 mg) and IFN-λ (0.5 μg) or 1×10^5 IU IFN-α were i.p. injected into mice on day 0, and then 0.5 μg IFN-λ or 1×10^5 IU of IFN-α was injected into mice on days 1, 2, and 4. On day 7, spleens were homogenized and stained with FITC CD8α Ab and PE-OVA tetramer for detecting OVA (SL8)-specific CD8$^+$ T cell population. For a negative control, PBS in place of IFN was injected on days 0, 1, 2, and 4. For a positive control, 100 μg polyI:C and OVA were injected into mice on day 0.

Results

TICAM-1 is essential for type III IFN production in response to polyI:C

DCs require the TLR3 adaptor TICAM-1 to produce type III IFN in response to polyI:C (15). Adding polyI:C to culture medium for mouse bone marrow–derived macrophages (BM-Mf) induced IFN-β, IFN-α2, IFN-α4, and IFN-λ2/3 mRNA expression, and TICAM-1 KO abolished IFN-λ2/3 mRNA expression (Supplemental Fig. 1A). These results suggested an essential role for TICAM-1 in type III IFN expression by BM-Mf.

Next, we examined cytokine mRNA expression in mouse tissues in response to i.p. injected polyI:C. IFN-β, IFN-α2, and IFN-α4 mRNA expression was detectable in both wild-type and TICAM-1 KO mice livers, whereas IFN-λ2/3 mRNA expression was not detected in TICAM-1 KO mouse liver (Supplemental Fig. 1B–1E). A recent study showed that TLR3 KO abolished IFN-λ serum levels in response to i.v. polyI:C injection (15). Our results and those in the previous study confirmed that TICAM-1 is essential for type III IFN expression in response to polyI:C.

IPS-1 plays a crucial role in type III IFN production in response to HCV in vivo

IPS-1 is essential for type I IFN production in response to HCV RNA and polyI:C in vivo (2, 3). We investigated whether IPS-1 could induce type III IFN production. An ectopic expression study using IPS-1 and TICAM-1 expression vectors showed that both TICAM-1 and IPS-1 activated the IFN-λ1 promoter (Supplemental Fig. 2A, 2B), which suggested that IPS-1 has the ability to induce IFN-λ1 expression. A deletion analysis showed that a 150- to 556-aa region of TICAM-1 and the transmembrane region of IPS-1 were essential for IFN-β, -λ1, and 2/3 promoter activations (Supplemental Fig. 2C, 2D).

Hydrodynamic injection is a highly efficient procedure to deliver nucleic acids to the mouse liver (21), and Gale Jr. and colleagues
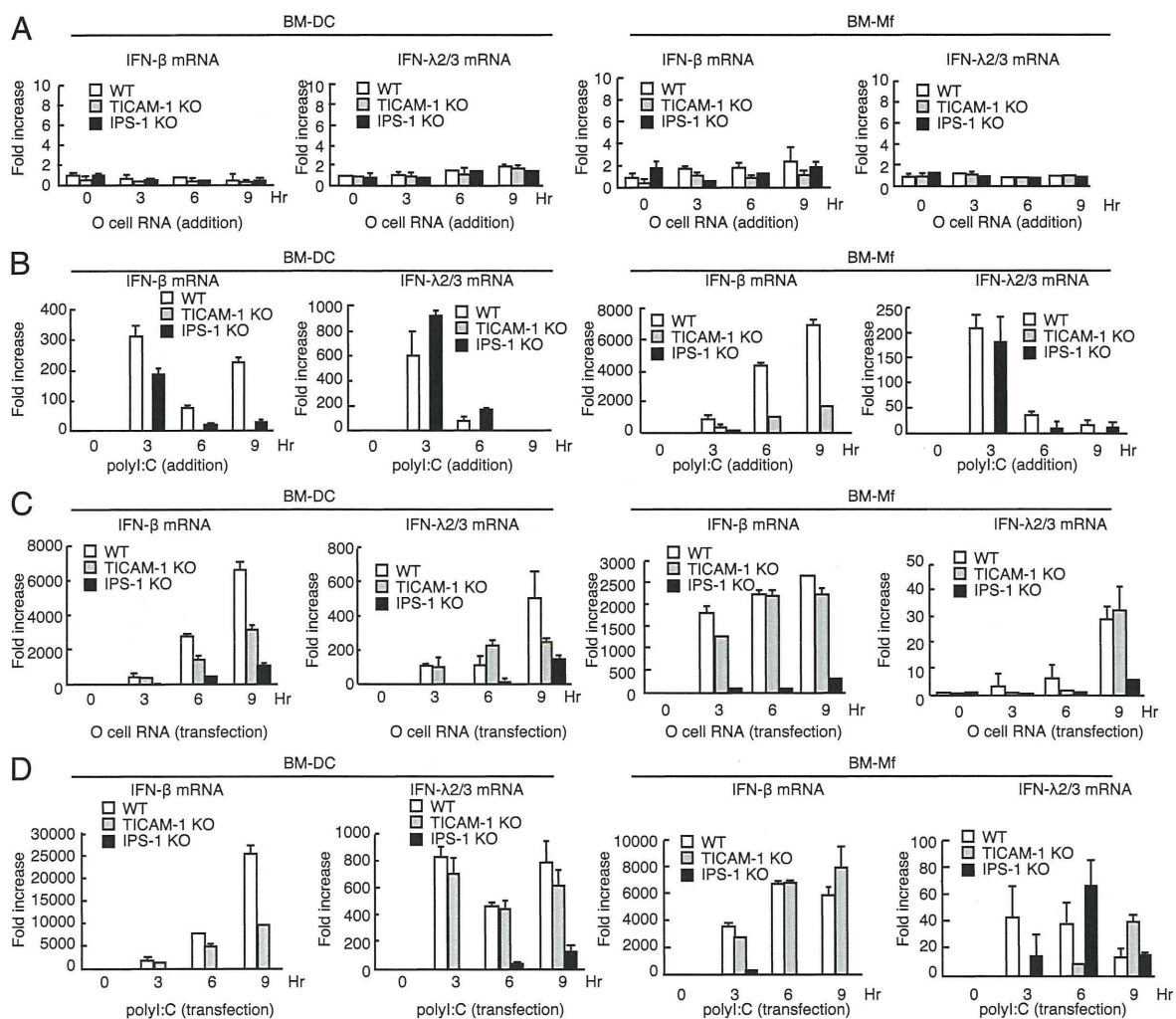

FIGURE 2. Type I and type III IFN expression in mouse DCs and Mfs in response to HCV RNA. (**A** and **B**) O cell RNA (A) or polyI:C (B) (20 μg) was added to the culture medium of BM-DCs and BM-Mfs derived from wild-type, TICAM-1 KO, and IPS-1 KO mice. IFN-β and IFN-λ2/3 mRNA levels were determined by quantitative RT-PCR at indicated hours. (**C** and **D**) O cell RNA (C) or polyI:C (D) (1 μg) was transfected into BM-DCs and BM-Mfs derived from wild-type, TICAM-1 KO, or IPS-1 KO mice. IFN-β (C) and -λ2/3 (D) mRNA levels were determined by quantitative RT-PCR.

(2) previously used a hydrodynamic assay to assess the role of RIG-I in type I IFN production in response to HCV RNA in vivo. Thus, to investigate the response to HCV RNA in vivo, we also used a hydrodynamic assay. We used RNA extracted from hepatocyte cell lines, O cells and Oc cells. O cells are derived from HuH-7 cells and contain HCV 1b full-length replicons (22). Oc cells were obtained by eliminating these replicons using IFN-α treatment (22). RNAs extracted from O cells (with HCV RNA) and Oc cells (without HCV RNA) were hydrodynamically injected into mouse livers, after which the cytokine expressions in mouse livers were determined. In wild-type mouse liver, O cell but not Oc cell RNA induced IFN-α2, β, and λ mRNA expression (Fig. 1A), which indicated that these cytokines were expressed in response to HCV RNAs within O cells that contained the HCV genome and replication intermediates in hepatocyte. Knockout of IPS-1 severely reduced IFN-β and α2 mRNA expressions in mouse liver in response to hydrodynamically injected O cell RNA (Fig. 1B). IFN-β protein level in mouse liver was also reduced by IPS-1 knockout (Fig. 1B). Although TICAM-1 was essential for IFN-λ2/3 mRNA expression in liver in response to i.p. injected polyI:C (Supplemental Fig. 1), TICAM-1 was dispensable for IFN-λ2/3 mRNA expression in response to hydrodynamically injected O cell RNA (Fig. 1B). In contrast, IPS-1 was essential for IFN-λ2/3 mRNA expression in response to hydrodynamically injected O cell RNA (Fig. 1B). A requirement for IPS-1 for IFN-λ2/3 mRNA expression in the liver was also found when in vitro synthesized HCV dsRNAs and ssRNAs were used for the hydrodynamic assay (Fig. 1C). These results suggested that IPS-1 plays a crucial role in type III IFN production in response to HCV RNA in vivo.

To corroborate the role of IPS-1 in type III IFN production, we next measured serum IFN-λ and -β levels in response to hydrodynamic injection of O cell RNA, HCV ssRNA, and HCV dsRNA. Interestingly, IPS-1 KO markedly reduced serum IFN-λ2/3 levels (Fig. 1D, 1E). Unexpectedly, TICAM-1 KO also reduced serum IFN-λ levels (Fig. 1D, 1E). Because TICAM-1 was dispensable for IFN-λ mRNA expression in the liver, it is possible that serum IFN-λ was produced from DCs in other tissues in a TICAM-1–dependent manner, as described below. Our data indicated that both TICAM-1 and IPS-1 are essential for type III IFN in response to HCV RNA in vivo. When polyI:C was hydrodynamically injected, knockout of TICAM-1 or IPS-1 moderately reduced IFN-λ2/3 levels in sera (Supplemental Fig. 3).

DCs produce type III IFN through an IPS-1–dependent pathway in response to cytoplasmic HCV RNA

HCV proteins and minus strands of its genome are detected in DCs and macrophages (Mfs) of chronically HCV-infected patients (23, 24), and recent study showed that DCs produce type I and III IFNs in response to HCV (17, 25). Thus, we assessed the role of IPS-1 in type III IFN production by DCs and Mfs in response to HCV RNA. Surprisingly, adding O cell RNA into the culture medium did not induce any IFN-β and -λ2/3 mRNA expression (Fig. 2A), whereas adding polyI:C into culture medium efficiently induced IFN-β and -λ2/3 mRNA expression (Fig. 2B), and TICAM-1 KO abolished the IFN-λ2/3 mRNA expression in bone marrow–derived DCs (BM-DCs) and BM-Mfs (Fig. 2B). It has been shown that polyI:C is preferentially internalized and activates TLR3 in human monocyte-derived DCs, whereas in vitro transcribed viral dsRNA hardly induced IFN-β production in monocyte-derived DCs (26). Thus, there is a possibility that, unlike polyI:C, TLR3 ligand in O cell RNA was not delivered to endosome where TLR3 is localized. Next, cells were stimulated with O cell RNA or polyI:C by transfection. BM-DCs and BM-Mfs expressed IFN-β and -λ2/3
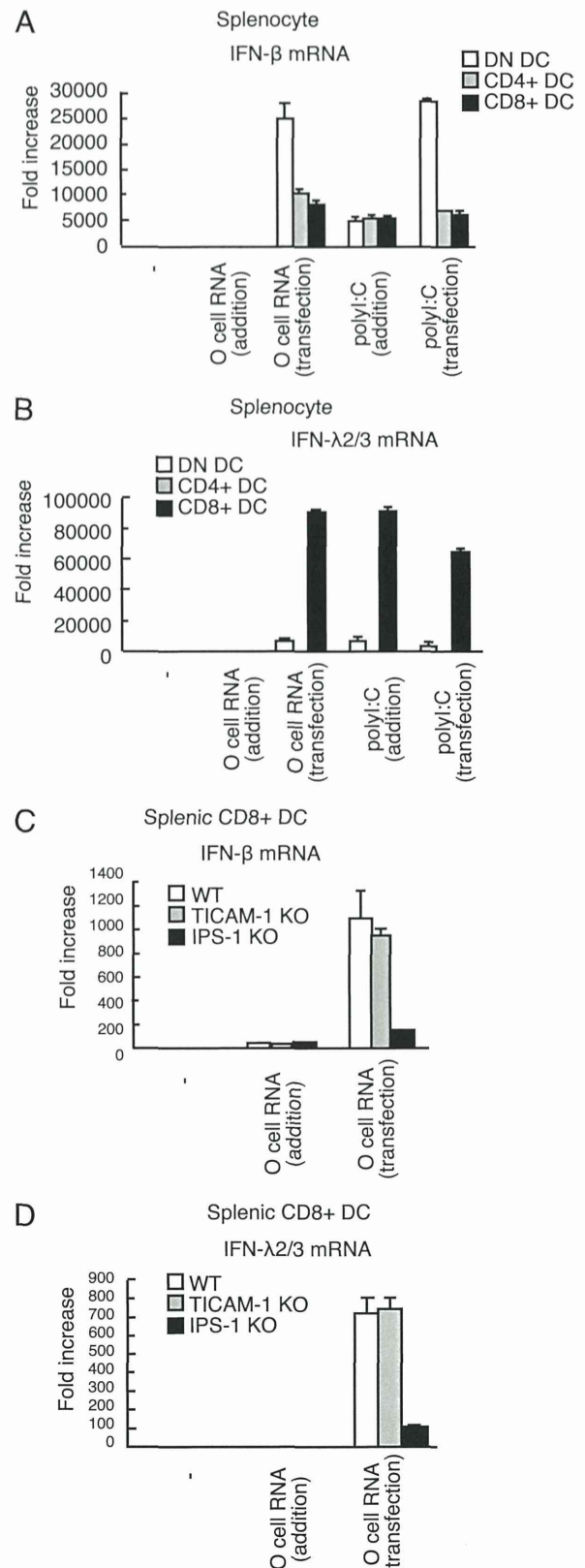
FIGURE 3. Type III IFN production by CD8^{+} DCs. (**A** and **B**) CD4^{+}, CD8^{+}, and DN DCs were isolated from mouse spleens and stimulated with 20 μg O cell RNA without transfection or stimulated with 1 μg O cell RNA by transfection for 6 h. IFN-β (A) and -λ2/3 (B) mRNA levels were determined by quantitative RT-PCR. (**C** and **D**) CD8^{+} DCs were isolated from wild-type, TICAM-1 KO, or IPS-1 KO mouse spleens. O cell RNA (20 μg) was added to the culture medium, or 1 μg O cell RNA was transfected into CD8^{+} DCs. Six hours after transfection, IFN-β (C) and -λ2/3 (D) mRNA levels were determined by quantitative RT-PCR.

mRNAs in response to O cell RNA and polyI:C (Fig. 2C, 2D). IPS-1 KO severely reduced IFN-λ2/3 mRNA expression in BM-DCs and BM-Mfs in response to O cell RNA (Fig. 2C). These results indicated that IPS-1 in BM-DCs and BM-Mfs plays a crucial role in IFN-λ2/3 mRNA expression in response to cytoplasmic HCV RNA.

Mice have CD4+, CD8+, and DN DCs. Thus, we next examined the IFN-β and -λ2/3 mRNA expression in these mouse DC subsets. As seen with BM-DCs, the mouse DCs expressed IFN-β and -λ2/3 mRNA in response to polyI:C but not O cell RNA in the culture medium, whereas stimulation with polyI:C or O cell RNA by transfection strongly induced their expression (Fig. 3A, 3B). Interestingly, CD8+ DCs highly expressed IFN-λ2/3 mRNA in response to stimulation with polyI:C or O cell RNA by transfection compared with CD4+ and DN DCs (Fig. 3A, 3B), and IPS-1 KO but not TICAM-1 KO severely reduced IFN-λ2/3 expression in CD8+ DCs in response to O cell RNA transfection (Fig. 3C, 3D). This indicated that IPS-1 was essential for IFN-λ2/3 mRNA expression in CD8+ DCs in response to cytoplasmic HCV RNA.

It was recently reported that exosomes mediate cell-to-cell transfer of HCV RNA from infected cells to cocultured DCs (27). We examined the production of IFN-β and -λ2/3 by CD8+ DCs that were cocultured with O cells and Oc cells. Coculture with O cells but not Oc cells induced IFN-β and -λ2/3 production by CD8+ DCs (Fig. 4A, 4B). Interestingly, TICAM-1 KO abolished IFN-λ2/3 mRNA expression and protein production, whereas IPS-1 KO failed to reduce IFN-λ2/3 mRNA expression and protein production in CD8+ DCs (Fig. 4C, 4D). This suggested that TICAM-1 but not IPS-1 was essential for IFN-λ2/3 production by CD8+ DCs when cocultured with hepatocytes with HCV replicons.

Type III IFN increases RIG-I expression in CD8+ DC

The receptor for type III IFN consists of IL-10RB and IL-28Rα subunits (8). DN and CD4+ DCs and NK cells did not express IL-28Rα mRNA, whereas CD8+ DCs expressed both IL-10RB and IL-28Rα mRNAs (Fig. 5A). Thus, we investigated the effects of IFN-λ on DC function.

First, we examined DC cell surface markers. Unlike IFN-α, IFN-λ3 hardly increased CD40, 80, and 86 surface marker expressions on CD8+ DCs (Fig. 5B). Second, we examined the effects of IFN-λ3 on cross-priming because CD8+ DCs have high cross-priming capability. OVA, IFN-α, and/or IFN-λ3 were i.p. injected into mice according to the indicated schedules (Fig. 5C). Seven days after injection, OVA (SL8)-specific CD8+ T cells in spleens were quantified by tetramer staining. For a positive control, OVA and polyI:C were i.p. injected into mice. The results showed that IFN-

λ3 failed to increase OVA-specific CD8+ T cells in the spleens and suggested that IFN-λ3 failed to promote cross-priming at least in our experimental condition (Fig. 5C).

Third, we examined NK cell activation by DCs. NK cells and DCs were isolated from mouse spleens and were cocultured for 24 h in the presence of IFN-α, λ3, or polyI:C. Although IFN-γ production was increased by IFN-α stimulation, IFN-λ3 failed to increase IFN-γ production (Fig. 5D). Next, we investigated a cell surface marker for NK cells when cocultured with DCs. The expression of CD69, a NK cell activation marker, was not increased by IFN-λ3 stimulation (Fig. 5E). These results indicated that, unlike IFN-α, IFN-λ3 failed to enhance the activation of NK cells by DCs.

Fourth, we investigated the expression of antiviral genes in CD8+ DCs in response to IFN-λ3 stimulation. Interestingly, IFN-λ3 stimulation increased RIG-I and Mx1 but not TLR3 mRNA expression in CD8+ DCs (Fig. 6A). In addition, pretreatment with IFN-λ3 augmented IFN-λ2/3 mRNA expression in CD8+ DCs in response to HCV RNA (Fig. 6B). Taken together, type III IFN induced RIG-I and antiviral protein expression but failed to promote DC-mediated NK cell activation and cross-priming.

Hepatocytes express type III IFN receptors. Thus, we examined the effects of IFN-λ on mouse hepatocytes. As with IFN-α, IFN-λ3 stimulation induced both TLR3 and RIG-I mRNA expression in mouse hepatocyte (Fig. 6C). Antiviral nucleases, ISG20 and RNaseL, and an IFN-inducible gene, Mx1, were induced by IFN-λ3 or IFN-α treatment (Fig. 6C). Pretreating mouse hepatocytes with IFN-λ3 enhanced IFN-β and -λ2/3 mRNA expression in response to stimulation with HCV RNA by transfection (Fig. 6D). These results indicated that IFN-λ3 induced cytoplasmic antivirus protein expression in mouse hepatocytes. We confirmed that IFN-λ3 treatment significantly reduced HCV RNA levels in O cells with HCV replicons (Fig. 6E). A previous study also reported that IFN-λ inhibits HCV replication (13).

Discussion

Previous studies have established the importance of the TLR3 pathway for type III IFN production in response to polyI:C (15) or HCV (17). In this study, we established the importance of IPS-1–dependent pathway for type III IFN production in response to cytoplasmic HCV RNA in vivo and in vitro using a mouse model. These data indicated that there are at least two main pathways for type III IFN production in vivo, as follows: one is TICAM-1 dependent, and the other is IPS-1 dependent.

We revealed that IFN-λ was efficiently produced by CD8+ DCs, the mouse counterpart of human BDCA3+ DCs, in response to
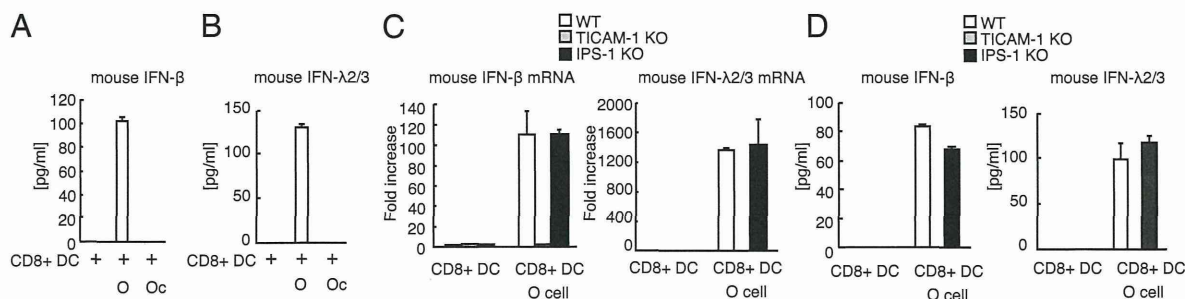
FIGURE 4. IFN-β and –λ production by CD8+ DCs cocultured with hepatocytes with HCV replicons. (**A** and **B**) CD8+ DCs isolated from wild-type spleens were cocultured with O cells (with HCV replicons) or Oc cells (without HCV replicons). After 24 h of coculture, IFN-β (A) and –λ2/3 (B) concentrations in culture medium were determined by ELISA. (**C**) CD8+ DCs isolated from wild-type, TICAM-1 KO, or IPS-1 KO spleens were cocultured with O cells with HCV replicons for six hours, and then IFN-β and –λ2/3 mRNA expression was determined by RT-qPCR. (**D**) CD8+ DCs isolated from wild-type, TICAM-1 KO, or IPS-1 KO spleens were cocultured with O cells with HCV replicons. IFN-β and –λ2/3 concentrations in culture medium were determined by ELISA.
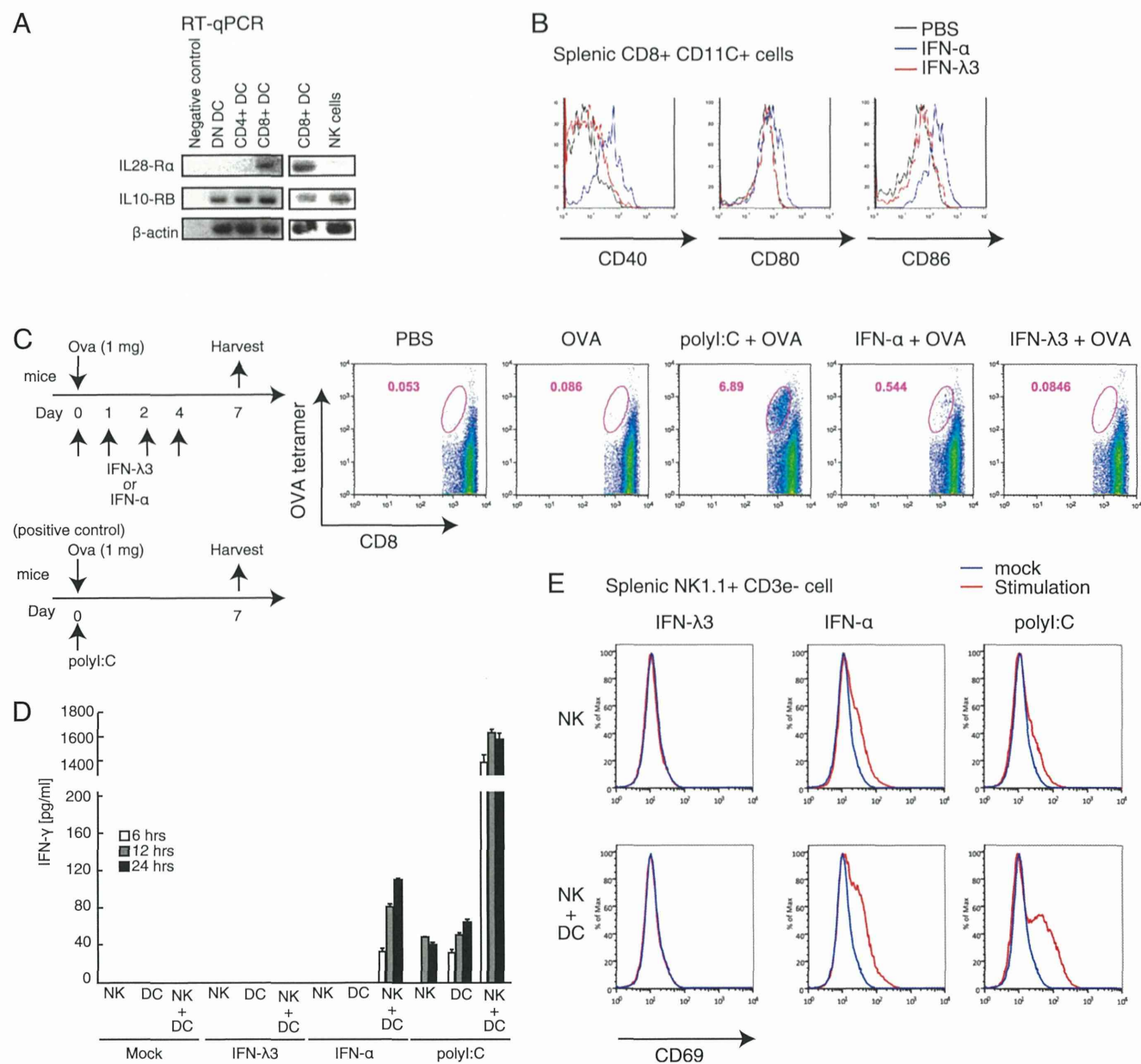
**FIGURE 5.** IFN-λ effects on DC functions. (**A**) DN, CD4⁺, CD8⁺ DCs, and NK cells were isolated from wild-type mouse spleens. IL-28Rα and IL-10RB mRNA were determined by RT-PCR. (**B**) A total of 0.5 μg IFN-λ3 or 1×10^5 IU IFN-α was i.p. injected into mice. Six hours after injection, spleen CD8⁺ DCs were isolated, and cell surface expressions of CD40, 80, and 86 were determined by FACS analysis. (**C**) OVA and IFN-λ or IFN-α were i.p. injected into mice on day 0, and then IFN-λ or IFN-α was injected into mice on days 1, 2, and 4. Spleens were excised on day 7, and OVA (SL8)-specific CD8⁺ T cells were determined by a tetramer assay. For a negative control, PBS in place of IFN was injected on days 0, 1, 2, and 4. For a positive control, polyI:C and OVA were injected into mice on day 0. (**D**) NK cells and CD11c⁺ DCs were isolated from mouse spleens and then stimulated with 1000 U/ml IFN-α, 100 ng/ml IFN-λ3, or 100 μg/ml polyI:C. IFN-γ concentrations in the culture medium at the indicated times were determined by ELISA. (**E**) NK cells were isolated from mouse spleens and then cultured with or without spleen CD11c⁺ DCs. Cells were stimulated with 1000 U/ml IFN-α, 100 ng/ml IFN-λ3, or 20 μg polyI:C. CD69 expression on NK cells was determined by FACS analysis.

cytoplasmic HCV RNA. Moreover, our data showed that IFN-λ stimulation increased the mRNA expression of RIG-I but not that of TLR3 in CD8⁺ DCs, and CD8⁺ DCs required IPS-1 to produce IFN-λ in response to stimulation with cytoplasmic HCV RNA. Furthermore, IFN-λ enhanced the mRNA expression of IFN-λ itself in CD8⁺ DCs, which suggested a positive feedback loop for IFN-λ mRNA expression in CD8⁺ DCs. IFN-λ failed to promote DC-mediated NK activation or cross-priming at least in our experimental conditions, whereas antiviral proteins, such as ISG20 and RNaseL, were efficiently induced by IFN-λ stimulation in hepatocytes and CD8⁺ DCs. These results established a novel role of IPS-1 in innate immune response against HCV via IFN-λ

production. IFN-λ pretreatment markedly increased IFN-β mRNA expression in response to HCV RNAs in mouse hepatocyte but not in CD8⁺ DCs (Fig. 6B, 6D). Although the underlying mechanism is unclear, it is possible that there is a cell-type–specific role of IFN-λ.

It was recently reported that BDCA3⁺ DCs require TLR3 for type III IFN production in response to cell-cultured HCV (17). They used a HCV 2a JFH1 strain that cannot infect human DCs in vitro (5). We also showed that the TLR3 adaptor TICAM-1 was essential for type III IFN production by CD8⁺ DCs when cocultured with O cells with HCV replicons. Thus, TLR3 appears to be essential for type III IFN production by DCs that are not infected with HCV. It
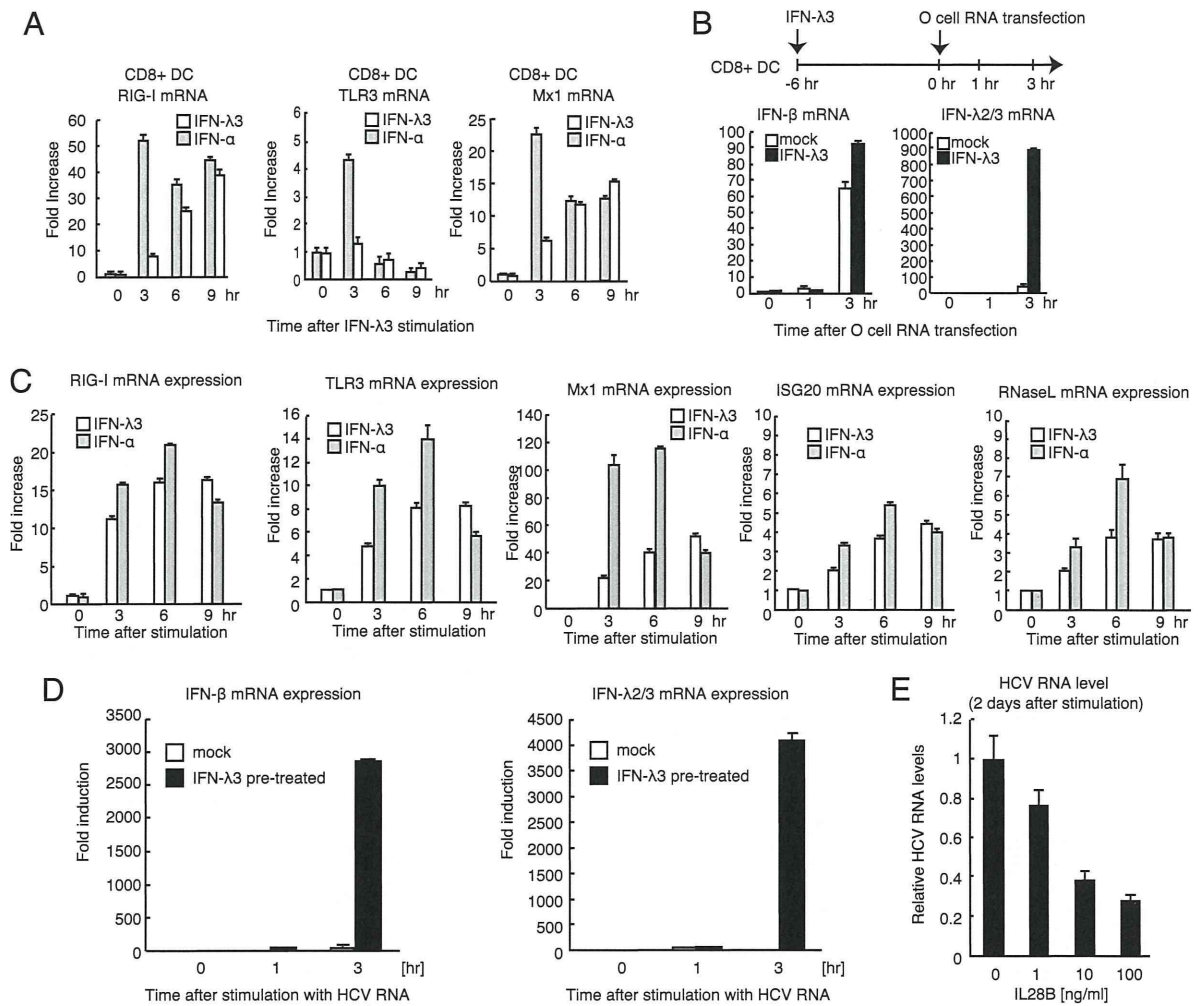
FIGURE 6. Antiviral responses induced by IFN-λ. (**A**) Mouse spleen CD8$^+$ DCs were stimulated with 100 ng/ml IFN-λ3 or 1000 IU/ml IFN-α, after which RIG-I, TLR3, and Mx1 mRNA levels were determined by quantitative RT-PCR. (**B**) Mouse spleen CD8$^+$ DCs were treated with 100 ng/ml IFN-λ3 for 6 h. O cell RNA was transfected into CD8$^+$ DCs, and IFN-β and -λ2/3 mRNA levels were determined by quantitative RT-PCR at the indicated times. (**C**) Mouse hepatocyte cell line cells were stimulated with 1000 U/ml IFN-α or 100 ng/ml IFN-λ3. RIG-I, TLR3, Mx1, ISG20, and RNaseL mRNA levels were determined by quantitative RT-PCR. (**D**) Mouse hepatocyte cell line cells were treated with 100 ng/ml IFN-λ3 for 6 h, and then O cell RNA was transfected into these cells. IFN-β and -λ2/3 mRNA levels were measured by quantitative RT-PCR at the indicated times. (**E**) O cells that contain HCV 1b full-length replicons were treated with human IL-28B at indicated concentration for 2 d. HCV RNA levels were determined by quantitative RT-PCR. HCV RNA levels were normalized to GAPDH mRNA expression.

has been shown that exosomes are internalized efficiently by DCs and sorted into early endosomes, where TLR3 is localized (28, 29). Unlike the transfected HCV RNA, exosome-enclosed HCV RNA might be efficiently sorted and released within early endosomes of CD8$^+$ DC, where TLR3 is localized, leading to TLR3-dependent IFN-λ2/3 production. Although HCV JFH1 infection particles fail to infect DCs in vitro, previous studies indicated that HCV infects DCs in chronically infected patients (23, 24, 30). In human patient DCs and hepatocytes infected with HCV, the IPS-1 pathway could play a pivotal role in type III IFN production.

Knockout of TICAM-1 failed to reduce IFN-λ2/3 mRNA expression in mouse liver after HCV RNA hydrodynamic injection, whereas knockout of TICAM-1 abolished IFN-λ2/3 levels in sera after HCV RNA hydrodynamic injection (Fig. 1B, 1D). Considering that there is a positive feedback loop for IFN-λ production, it is possible that TICAM-1 and IPS-1 pathways augment IFN-λ production each other in vivo; however, we do not exclude a possibility that TICAM-1 is involved in posttranscriptional step of IFN-λ production.

HCV NS3-4A protease cleaves IPS-1 to suppress host innate immune responses (31, 32). However, it is notable that a mutation

within the *RIG-I* gene in HuH7.5 cells increases cellular permissiveness to HCV infection (33). This indicates that the RIG-I pathway is functional at least during the early phase of HCV infection before NS3-4A cleaves IPS-1. Thus, we propose that IPS-1 is important for type III IFN production during the early phase of HCV infection.

IFN-α augmented DC-mediated NK cell activation and cross-priming, whereas IFN-λ failed to augment DC-mediated NK cell activation and cross-priming in our experimental conditions. However, as seen with IFN-α, IFN-λ could induce RNaseL and ISG20 mRNA expression. These data indicated that IFN-λ induces cytoplasmic antiviral proteins to eliminate infected virus. A previous study showed that IPS-1 is required for initial antiviral response but dispensable for the protective adaptive immune response to influenza A virus (34). Thus, it is expected that IPS-1–mediated IFN-λ production would be required for initial antiviral response to HCV infection.

In summary, our results provide insights into type III IFN production mechanism in response to HCV RNA in vivo and identify IPS-1 as a molecule crucial for producing type III IFN from hepatocyte and CD8$^+$ DCs in response to cytoplasmic HCV RNA.

Acknowledgments

Disclosures

References

1. Lauer, G. M., and B. D. Walker. 2001. Hepatitis C virus infection. N. Engl. J. Med. 345: 41–52.
2. Saito, T., D. M. Owen, F. Jiang, J. Marcotrigiano, and M. Gale, Jr. 2008. Innate immunity induced by composition-dependent RIG-I recognition of hepatitis C virus RNA. Nature 454: 523–527.
3. Kumar, H., T. Kawai, H. Kato, S. Sato, K. Takahashi, C. Coban, M. Yamamoto, S. Uematsu, K. J. Ishii, O. Takeuchi, and S. Akira. 2006. Essential role of IPS-1 in innate immune responses against RNA viruses. J. Exp. Med. 203: 1795–1803.
4. Matsumoto, M., and T. Seya. 2008. TLR3: interferon induction by double-stranded RNA including poly(I:C). Adv. Drug Deliv. Rev. 60: 805–812.
5. Ebihara, T., M. Shingai, M. Matsumoto, T. Wakita, and T. Seya. 2008. Hepatitis C virus-infected hepatocytes extrinsically modulate dendritic cell maturation to activate T cells and natural killer cells. Hepatology 48: 48–58.
6. Yamamoto, M., S. Sato, H. Hemmi, K. Hoshino, T. Kaisho, H. Sanjo, O. Takeuchi, M. Sugiyama, M. Okabe, K. Takeda, and S. Akira. 2003. Role of adaptor TRIF in the MyD88-independent Toll-like receptor signaling pathway. Science 301: 640–643.
7. Oshiumi, H., M. Matsumoto, K. Funami, T. Akazawa, and T. Seya. 2003. TICAM-1, an adaptor molecule that participates in Toll-like receptor 3-mediated interferon-beta induction. Nat. Immunol. 4: 161–167.
8. Sheppard, P., W. Kindsvogel, W. Xu, K. Henderson, S. Schlutsmeyer, T. E. Whitmore, R. Kuestner, U. Garrigues, C. Birks, J. Roraback, et al. 2003. IL-28, IL-29 and their class II cytokine receptor IL-28R. Nat. Immunol. 4: 63–68.
9. Thomas, D. L., C. L. Thio, M. P. Martin, Y. Qi, D. Ge, C. O'Huigin, J. Kidd, K. Kidd, S. I. Khakoo, G. Alexander, et al. 2009. Genetic variation in IL28B and spontaneous clearance of hepatitis C virus. Nature 461: 798–801.
10. Tanaka, Y., N. Nishida, M. Sugiyama, M. Kurosaki, K. Matsuura, N. Sakamoto, M. Nakagawa, M. Korenaga, K. Hino, S. Hige, et al. 2009. Genome-wide association of IL28B with response to pegylated interferon-alpha and ribavirin therapy for chronic hepatitis C. Nat. Genet. 41: 1105–1109.
11. Suppiah, V., M. Moldovan, G. Ahlenstiel, T. Berg, M. Weltman, M. L. Abate, M. Bassendine, U. Spengler, G. J. Dore, E. Powell, et al. 2009. IL28B is associated with response to chronic hepatitis C interferon-alpha and ribavirin therapy. Nat. Genet. 41: 1100–1104.
12. Ge, D., J. Fellay, A. J. Thompson, J. S. Simon, K. V. Shianna, T. J. Urban, E. L. Heinzen, P. Qiu, A. H. Bertelsen, A. J. Muir, et al. 2009. Genetic variation in IL28B predicts hepatitis C treatment-induced viral clearance. Nature 461: 399–401.
13. Marcello, T., A. Grakoui, G. Barba-Spaeth, E. S. Machlin, S. V. Kotenko, M. R. MacDonald, and C. M. Rice. 2006. Interferons alpha and lambda inhibit hepatitis C virus replication with distinct signal transduction and gene regulation kinetics. Gastroenterology 131: 1887–1898.
14. Le Bon, A., N. Etchart, C. Rossmann, M. Ashton, S. Hou, D. Gewert, P. Borrow, and D. F. Tough. 2003. Cross-priming of CD8+ T cells stimulated by virus-induced type I interferon. Nat. Immunol. 4: 1009–1015.
15. Lauterbach, H., B. Bathke, S. Gilles, C. Traidl-Hoffmann, C. A. Luber, G. Fejer, M. A. Freudenberg, G. M. Davey, D. Vremec, A. Kallies, et al. 2010. Mouse CD8alpha+ DCs and human BDCA3+ DCs are major producers of IFN-lambda in response to poly IC. J. Exp. Med. 207: 2703–2717.
16. Schulz, O., S. S. Diebold, M. Chen, T. I. Näslund, M. A. Nolte, L. Alexopoulou, Y. T. Azuma, R. A. Flavell, P. Liljeström, and C. Reis e Sousa. 2005. Toll-like receptor 3 promotes cross-priming to virus-infected cells. Nature 433: 887–892.
17. Yoshio, S., T. Kanto, S. Kuroda, T. Matsubara, K. Higashitani, N. Kakita, H. Ishida, N. Hiramatsu, H. Nagano, M. Sugiyama, et al. 2013. Human blood dendritic cell antigen 3 (BDCA3)(+) dendritic cells are a potent producer of interferon-λ in response to hepatitis C virus. Hepatology 57: 1705–1715.
18. Oshiumi, H., M. Okamoto, K. Fujii, T. Kawanishi, M. Matsumoto, S. Koike, and T. Seya. 2011. The TLR3/TICAM-1 pathway is mandatory for innate immune responses to poliovirus infection. J. Immunol. 187: 5320–5327.
19. Aly, H. H., H. Oshiumi, H. Shime, M. Matsumoto, T. Wakita, K. Shimotohno, and T. Seya. 2011. Development of mouse hepatocyte lines permissive for hepatitis C virus (HCV). PLoS One 6: e21284.
20. Oshiumi, H., M. Ikeda, M. Matsumoto, A. Watanabe, O. Takeuchi, S. Akira, N. Kato, K. Shimotohno, and T. Seya. 2010. Hepatitis C virus core protein abrogates the DDX3 function that enhances IPS-1-mediated IFN-beta induction. PLoS One 5: e14258.
21. Liu, F., Y. Song, and D. Liu. 1999. Hydrodynamics-based transfection in animals by systemic administration of plasmid DNA. Gene Ther. 6: 1258–1266.
22. Ikeda, M., K. Abe, H. Dansako, T. Nakamura, K. Naka, and N. Kato. 2005. Efficient replication of a full-length hepatitis C virus genome, strain O, in cell culture, and development of a luciferase reporter system. Biochem. Biophys. Res. Commun. 329: 1350–1359.
23. Goutagny, N., A. Fatmi, V. De Ledinghen, F. Penin, P. Couzigou, G. Inchauspé, and C. Bain. 2003. Evidence of viral replication in circulating dendritic cells during hepatitis C virus infection. J. Infect. Dis. 187: 1951–1958.
24. Sansonno, D., A. R. Iacobelli, V. Cornacchiulo, G. Iodice, and F. Dammacco. 1996. Detection of hepatitis C virus (HCV) proteins by immunofluorescence and HCV RNA genomic sequences by non-isotopic in situ hybridization in bone marrow and peripheral blood mononuclear cells of chronically HCV-infected patients. Clin. Exp. Immunol. 103: 414–421.
25. Stone, A. E., S. Giugliano, G. Schnell, L. Cheng, K. F. Leahy, L. Golden-Mason, M. Gale, Jr., and H. R. Rosen. 2013. Hepatitis C virus pathogen associated molecular pattern (PAMP) triggers production of lambda-interferons by human plasmacytoid dendritic cells. PLoS Pathog. 9: e1003316.
26. Itoh, K., A. Watanabe, K. Funami, T. Seya, and M. Matsumoto. 2008. The clathrin-mediated endocytic pathway participates in dsRNA-induced IFN-beta production. J. Immunol. 181: 5522–5529.
27. Dreux, M., U. Garaigorta, B. Boyd, E. Décembre, J. Chung, C. Whitten-Bauer, S. Wieland, and F. V. Chisari. 2012. Short-range exosomal transfer of viral RNA from infected cells to plasmacytoid dendritic cells triggers innate immunity. Cell Host Microbe 12: 558–570.
28. Morelli, A. E., A. T. Larregina, W. J. Shufesky, M. L. Sullivan, D. B. Stolz, G. D. Papworth, A. F. Zahorchak, A. J. Logar, Z. Wang, S. C. Watkins, et al. 2004. Endocytosis, intracellular sorting, and processing of exosomes by dendritic cells. Blood 104: 3257–3266.
29. Matsumoto, M., K. Funami, M. Tanabe, H. Oshiumi, M. Shingai, Y. Seto, A. Yamamoto, and T. Seya. 2003. Subcellular localization of Toll-like receptor 3 in human dendritic cells. J. Immunol. 171: 3154–3162.
30. Pham, T. N., S. A. MacParland, P. M. Mulrooney, H. Cooksley, N. V. Naoumov, and T. I. Michalak. 2004. Hepatitis C virus persistence after spontaneous or treatment-induced resolution of hepatitis C. J. Virol. 78: 5867–5874.
31. Meylan, E., J. Curran, K. Hofmann, D. Moradpour, M. Binder, R. Bartenschlager, and J. Tschopp. 2005. Cardif is an adaptor protein in the RIG-I antiviral pathway and is targeted by hepatitis C virus. Nature 437: 1167–1172.
32. Li, X. D., L. Sun, R. B. Seth, G. Pineda, and Z. J. Chen. 2005. Hepatitis C virus protease NS3/4A cleaves mitochondrial antiviral signaling protein off the mitochondria to evade innate immunity. Proc. Natl. Acad. Sci. USA 102: 17717–17722.
33. Saito, T., R. Hirai, Y. M. Loo, D. Owen, C. L. Johnson, S. C. Sinha, S. Akira, T. Fujita, and M. Gale, Jr. 2007. Regulation of innate antiviral defenses through a shared repressor domain in RIG-I and LGP2. Proc. Natl. Acad. Sci. USA 104: 582–587.
34. Koyama, S., K. J. Ishii, H. Kumar, T. Tanimoto, C. Coban, S. Uematsu, T. Kawai, and S. Akira. 2007. Differential role of TLR- and RLR-signaling in the immune responses to influenza A virus infection and vaccination. J. Immunol. 179: 4711–4720.
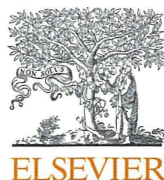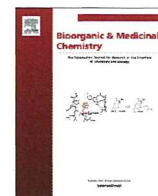
Synthesis of 3′,4′-difluoro-3′-deoxyribonucleosides and its evaluation of the biological activities: Discovery of a novel type of anti-HCV agent 3′,4′-difluorocordycepin

CrossMark

Hisashi Shimada [a], Kazuhiro Haraguchi [b,*], Kumi Hotta [a], Tomoko Miyaike [a], Yasuyuki Kitagawa [c], Hiromichi Tanaka [a], Ryutaro Kaneda [d], Hiroshi Abe [d], Satoshi Shuto [d], Kyoko Mori [e], Youki Ueda [e], Nobuyuki Kato [e], Robert Snoeck [f], Graciela Andrei [f], Jan Balzarini [f]

[a] School of Pharmacy, Showa University, 1-5-8 Hatanodai, Shinagawa-ku, Tokyo 142-8555, Japan
[b] Nihon Pharmaceutical University, 10281 Komuro, Inamachi, Kita-adachi-gun, Saitama 362-0806, Japan
[c] Yokohama College of Pharmacy, 601 Matano-cho, Totsuka-ku, Yokohama-shi, Kanagawa 245-0066, Japan
[d] Faculty of Pharmaceutical Sciences, Hokkaido University, Kita-12, Nishi-6, Kita-ku, Sapporo 060-0812, Japan
[e] Department of Tumor Virology, Okayama University Graduate School of Medicine, Dentistry, and Pharmaceutical Sciences, 2-5-1 Shikata-cho, Okayama 700-8558, Japan
[f] Rega Institute for Medical Research, Katholieke Universiteit Leuven, Minderbroedersstraat 10, B-3000 Leuven, Belgium

ARTICLE INFO

ABSTRACT

Upon reacting 3′,4′-unsaturated cytosine (8 and 9) and adenine nucleosides (13 and 14) with XeF_2/$BF_3 \cdot OEt_2$, the respective novel 3′,4′-difluoro-3′-deoxyribofuranosyl nucleosides (10–12 and 15–18) could be obtained. Formation of anti-adducts (11, 16 and 18) revealed that the fluorination involved oxonium ions as incipient intermediates. TBDMS-protected 3′,4′-unsaturated adenosine provided the β-face adducts as sole stereoisomers whereas α-face-selectivity was observed with the TBDPS-protected adenosine 14. The evaluation of the novel 3′-deoxy-3′,4′-difluororibofuranosylcytosine-(19–21) and adenine nucleosides (22–25) against antitumor and antiviral activities revealed that 3′,4′-difluorocordycepin (24) was found to possess anti-HCV activity. The SI of 24 was comparable to that of the anti-HCV drug ribavirin. However, sofosbuvir, FDA-approved novel anti-HCV drug, showed better SI value. Our finding revealed that the introduction of the fluoro-substituent into the 4′-position of cordycepin derivatives decreased the cytotoxicity to the host cell with retention of the antiviral activity.

© 2014 Elsevier Ltd. All rights reserved.

1. Introduction

Nucleoside analogues are recognized as an important class of biologically active compounds, especially as antiviral and antitumor agents.[1–4] Among their sugar-modified analogues, fluorinated sugar nucleosides have attracted much attention due to their remarkable antiviral and antitumor activities.[5a] In Figure 1, a selection of antibacterial, antiviral and antitumor derivatives is depicted. Nucleocidin (1) is an antitrypanosomal nucleoside antibiotic and its core structure is 4′-fluoroadenosine. FLT (2) is a synthetic 3′-monofluorinated 3′-deoxythymidine and exhibits anti-HIV activity. 2′-β-Fluorinated thymidine nucleoside, FMAU (3a), has been known to possess antiherpes activity. Quite recently, FDA has approved sofosbuvir (3b), 2′-deoxy-2′-α-fluoro-2′-β-C-methylurodine, for the treatment of chronic hepatitis C.[5b]

Other than monofluoro-sugar derivatives, nucleosides substituted with two fluoro groups in the sugar moiety have been synthesized and evaluated for biological activities. One type of these is the geminally-difluorinated nucleosides, which are depicted in Figure 2. 2′,2′-Geminally-difluorinated 2′-deoxycytidine (gemicitabine, 4) has been well known for treatment of pancreatic cancer.[5a] Its regioisomer, 3′,3′-geminally-difluorinated 3′-deoxycytidine (5a) and thymidine derivative (5b) have also been synthesized.[5a] Another type of difluoro nucleosides are the vicinally-difluorinated derivatives. Four possible isomers (I–IV) have been reported[6] and among them, 2′,3′-dideoxy-2′,3′-difluoro-β-D-arabinofuranosyl cytosine (6) has been reported to show anti-HIV activity (Fig. 3).[7]

In this context, we have been interested in the synthesis and biological evaluation of novel 3′,4′-difluorinated nucleosides V because the respective adenine nucleosides VI are 3′,4′-difluorinated analogues of the nucleoside antibiotic cordycepin[8] (Fig. 4).

A synthetic plan for the target molecules is illustrated in Scheme 1. In the course of our ongoing research on the synthetic chemistry of unsaturated sugar nucleosides,[9] we have already
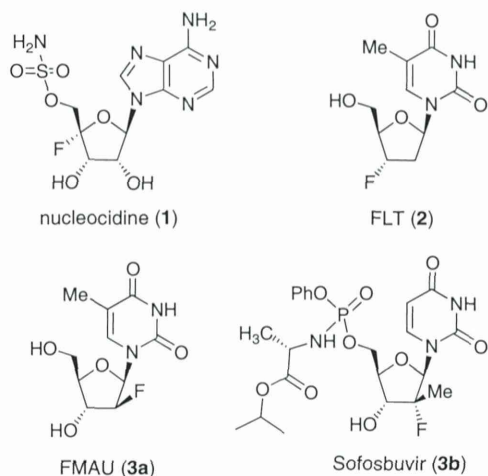
Figure 1. Structure of biologically-active monofluoro compounds 1–3.
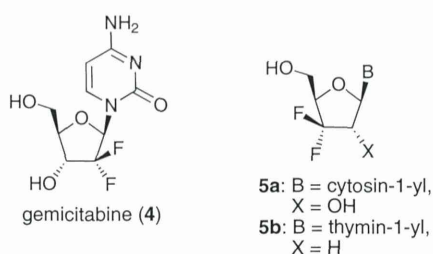

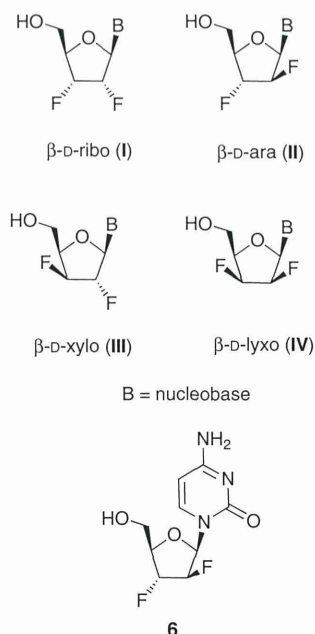Figure 2. Structure of geminally-difluorinated compounds 4–5.

Figure 3. Structure of 2′,3′-vicinal-difluoronucleosides I–IV and anti-HIV agent 6.

reported on the allylic rearrangement of 3′,4′-unsaturated nucleosides leading to 4′-substituted 2′,3′-didehydro-2′,3′-dideoxynucleosides.[10] Aiming at expanding the synthetic utility of 3′,4′-unsaturated nucleosides (VII), we have intended to utilize VII as a substrate for the synthesis of the target molecules. It has been demonstrated that xenon difluoride (XeF$_2$) is a reagent for the

fluorination of unsaturated organic molecules under mild reaction conditions.[11] In the case of alkenes as substrates, 1,2-difluoroalkanes could be obtained.[12] This synthetic method has also been applied to acetylglycal leading to 1,2-difluoro-1,2-dideoxyhexoses.[13,14] We thus envisioned that xenon difluoride-mediated difluorination of 3′,4′-unsaturated nucleosides (VII) would give rise to unprecedented vicinal difluoronucleosides, 3′-deoxy-3′,4′-difluoro-ribonucleoside (VIII). In this paper, we will describe these results and the biological activities of VIII.

2. Results and discussion

2.1. Chemistry

Initially, the di-fluorination of 3′,4′-unsaturated cytosine nucleosides was examined. The substrates 8 and 9 were prepared from 7[10] through de-acetylation and silylation of the resulting diols (Scheme 2). When a benzene solution of BF$_3$·OEt$_2$ (3.0 equiv) was added to an Et$_2$O solution of 8 and XeF$_2$ (1.5 equiv) at 0 °C under Ar atmosphere, the desired vicinal difluorination proceeded and a mixture of the respective 3′-deoxy-3′,4′-difluorocytidine derivatives IX (Pg = TBDMS) was obtained (Scheme 3). To separate these stereoisomers, the silyl-protecting groups were converted into acetyl groups in a one pot manner, and the β-syn-adduct 10 (α-L-arabinofuranosyl isomer) and β-anti-adduct 11 (β-D-xylofuranosyl isomer) could be obtained in 25% and 27% yields, respectively (Table 1, entry 1). The depicted structures were assigned on the basis of NOE experiments; for 10, H-1′/H-3′ (2.1%) and H-3′/H-5′b (1.1%); for 11 H-1′/H-3′ (0.7%) and H-5′a/H-6 (0.6%). In the ^{1}H NMR spectra of 10 and 11, the most significant difference was the coupling pattern of the C1′ proton. Thus, 10 showed vicinal and five-bond long-range coupling ($J_{1',2'} = J_{1',4'F} \approx 6.4$ Hz) whereas 9 showed only a small vicinal coupling ($J_{1',2'} = 2.4$ Hz). It has been reported that five-bond H–F coupling ($J_{F1,H4} = 6$–7 Hz) occurs in pentofuranosyl fluorides when the C1-F and C4-H functions are trans disposed, whereas the corresponding cis isomers show much smaller values (1–2 Hz).[15,16] This report supported the depicted structures of 10 and 11. Another characteristic difference was the observed four-bond long-range H-F coupling between C5′-H and C3′-F ($J_{F3',H5'a} = 2.0$ Hz and $J_{F3',H5'b} = 2.8$ Hz) in 11 (H-5′a and H-5′b coupled as ddd, respectively); this was observed when C5′ and C3-F are in a cis relationship. On the other hand, no such long-range coupling was observed in 10 (H-5′a and H-5′b appeared as dd) in which C5′ and C3′-F are trans disposed.

The stereochemical outcome of the di-fluorination could be rationalized by shielding the α-face of the 3′,4′-double bond with the sterically encumbered 2′-O-TBDMS group leading to the formation of the incipient β-coordinated transition state X and subsequently-formed oxonium ion XI (Fig. 5).

When TBDPS-protected 9 was subjected to the fluorination under the same reaction conditions as for 8, α-syn adduct 12 (β-D-ribofuranosyl isomer) was obtained in 5% isolated yield along with 10 (52%) and 11 (34%) after removal of the TBDPS groups of IX (Pg = TBDPS) and acetylation of the resulting diols (Scheme 3 and entry 2 in Table 1). In the ^{1}H NMR spectrum of 12, the anomeric proton appeared as a doublet and the C5′-proton was observed as a double doublet. Finally, the depicted structure was supported by NOE experiments; H-6/ H-3′ (0.7%), H-6/H-5′b (1.0%), H-2′/H-3′ (5.1%) and H-5′a/ H-3′ (0.5%). The formation of the α-adduct could be explained by the out-side orientation of the 2′-O-TBDPS group to the double bond caused by a buttressing effect of the 5′-O-TBDPS group and the 2′-O-TBDPS group.
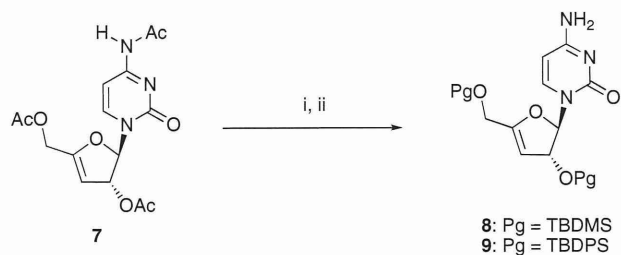
Next, the difluorination of the TBDMS-protected adenine nucleoside 13[17] was examined (Scheme 4). Under the above-mentioned reaction conditions, 13 gave a mixture of two stereoisomers XII (Pg = TBDMS). The mixture was subjected to N^6-pivaloylation,
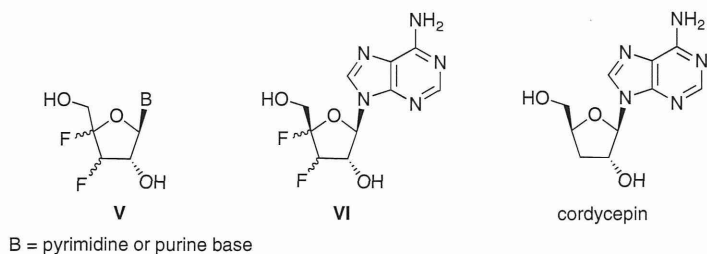
Figure 4. Structure of 3′,4′-difluoronucleoside (**V** and **VI**) and cordycepin.
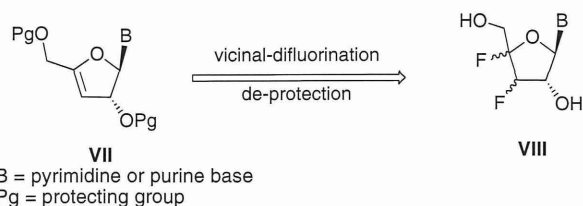
Scheme 1. Synthesis of 3′,4′-difluoronucleosides (**VIII**) from 3′,4′-unsaturated nucleosides (**VII**).

Table 1
XeF₂-mediated difluorination of 3′,4′-unsaturated cytidine and adenosine derivatives **8, 9, 13** and **14**

Entry	Substrate	Products (isolated yields, %)				β/α
		β-syn	β-anti	α-syn	α-anti	
1	**8**	**10** (25)	**11** (27)	–	–	1/0
2	**9**	**10** (52)	**11** (34)	**12** (5)	–	1/0.06
3	**13**	**15** (45)	**16** (22)	–	–	1/0
4	**14**	**15** (18)	**16** (2)	**17** (36)	**18** (5)	1/2.1

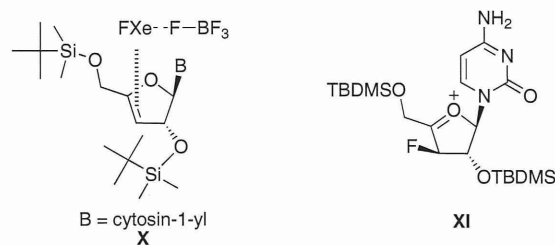
Scheme 2. Synthesis of 3′,4′-unsaturated cytidines **8** and **9**. Reactions and conditions: (i) NH₃/MeOH; (ii) TBDMSCl or TBDPSCl /imidazole/DMF; **8** (65%), **9** (71%).
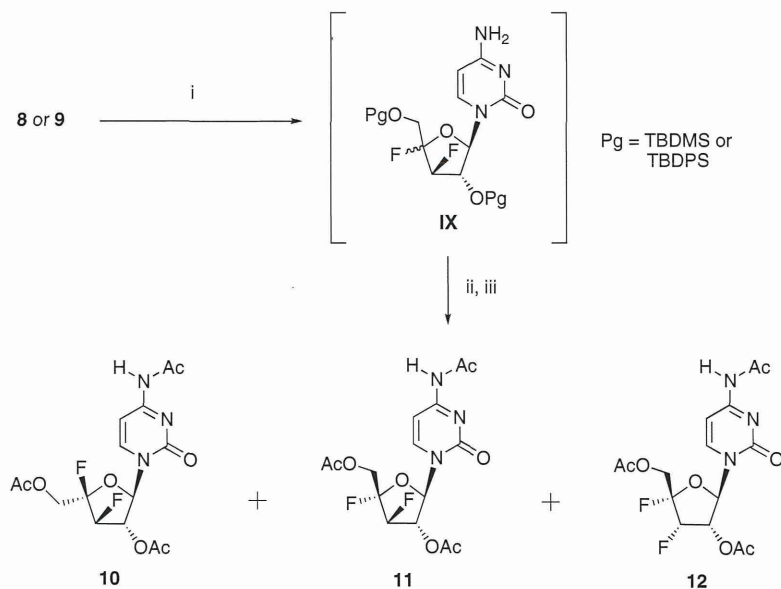

Figure 5. Plausible transition state **X** and oxonium ion **XI** in the fluorination of **8**.

Scheme 3. Reaction of 3′,4′-unsaturated cytidines **8** and **9** with XeF₂/BF₃·OEt₂: Formation of **10, 11** and **12**. Reactions and conditions: (i) XeF₂, BF₃·OEt₂, ether–benzene; (ii) Bu₄NF/THF; (iii) Ac₂O.